MATHEMATICAL BIOSCIENCES
AND ENGINEERING
Volume **13**, Number **3**, June **2016**

doi:10.3934/mbe.2016002

pp. **483–493**

A LEAKY INTEGRATE-AND-FIRE MODEL WITH ADAPTATION FOR THE GENERATION OF A SPIKE TRAIN

Aniello Buonocore, Luigia Caputo and Enrica Pirozzi

Dipartimento di Matematica e Applicazioni
Università di Napoli Federico II, Via Cintia, Napoli, Italy

Maria Francesca Carfora

Istituto per le Appplicazioni del Calcolo "Mauro Picone"
Consiglio Nazionale delle Ricerche, Via Pietro Castellino, Napoli, Italy

Abstract. A model is proposed to describe the spike-frequency adaptation observed in many neuronal systems. We assume that adaptation is mainly due to a calcium-activated potassium current, and we consider two coupled stochastic differential equations for which an analytical approach combined with simulation techniques and numerical methods allow to obtain both qualitative and quantitative results about asymptotic mean firing rate, mean calcium concentration and the firing probability density. A related algorithm, based on the Hazard Rate Method, is also devised and described.

1. **Introduction.** Spike-frequency adaptation is a ubiquitous phenomenon in the central nervous system, that may play a prominent role in neural information processing. One of the first attempts to investigate the adaptation of discharge frequency in repetitive firing neurons is due to Granit et al. [15]; they found a brief phase of "adaptation"preceding the steady state of firing, in which the impulse frequency diminishes at a rate varying from cell to cell and depending on intensity. They also noted that at the beginning of adaptation, during the release of initial spikes, after-hyperpolarization develops and contributes to the adaptive process by diminishing the firing rate. However, the functional role of adaptation is still not completely clear. Crook et al [10] showed in a theoretical framework that spike frequency adaptation in a small network of cortical neurons stabilized the synchronous behaviour with mutual excitation. Ermentrout et al [12] explored the role of adaptation in enhancing the synchronization properties of cortical neurons. Also Fuhrmann et al. [14] suggested that adaptation could be one of the crucial factors in setting the frequency of population rhythms in the neocortex. Other possible roles have been suggested, including the phenomena of forward masking and selective attention [22], when the neuronal response to subsequent or weaker inputs is inhibited.

There is a large variety of mechanisms responsible for firing rate adaptation. The prominent ones are the ionic currents related to the voltage-dependent potassium

2010 *Mathematics Subject Classification.* Primary: 60J60; Secondary: 60H35.

Key words and phrases. Calcium-activated potassium current, fast-slow analysis, hazard rate method.

This work has been performed under partial support by Project "Metodi, Modelli, Algoritmi e Software per le Scienze di Base ed Applicate", Dipartimento di Matematica e Applicazioni "Renato Caccioppoli", Università degli Studi di Napoli Federico II.

channels (M-type currents, [3]), further those related to the slow calcium dependent potassium channels (AHP currents, [23, 25, 28]) and those responsible for the recovery from inactivation of the sodium channel [13]. Benda and Herz [1] suggested that all these different adaptation mechanisms could be described by a generic voltage gated current as introduced by Hodgkin and Huxley [17] so to derive a "universal" model independent of the biophysical processes underlying adaptation.

Despite that detailed conductance-based neuron models of the Hodgkin-Huxley type [16, 17] explicitly considering many ion channels have been proposed, their complexity strongly limits their applicability. On the other hand, simplified phenomenological models as the stochastic leaky integrate-and-fire (LIF) one [27, 31] are certainly less exact, but mathematically more tractable. It has been shown [29, 30] that the classical LIF model is unable to reproduce some high order statistics of the observed interspike intervals (ISIs). However, generalized LIF models are still able to give an effective description of neural activity, reproducing the observed spiking behavior [2, 14, 19, 20]. Finally, such low-dimensional simplified models are well suited for network simulations and can be a useful tool to explore the role of adaptation on the systems level [10].

The generalization of a LIF model to include spike-frequency adaptation is often realized by coupling the equation for the evolution of the membrane potential to an equation for the dynamics of a given ion species. After each spike, due to the opening and closing of specific gates, the intracellular concentration of that species is abruptly modified and then decays to its resting value; as a consequence, a resulting ion-dependent current affects the discharge rate ([22, 26]). Alternative models assume that adaptation is generated by a dynamically varying firing threshold: such a threshold is transiently elevated following a spike and subsequently decays until the next spike is generated ([9, 18, 21]).

In the present work we consider a model inspired by the work of Liu and Wang [22]. We assume that adaptation is provoked mainly by a calcium-activated potassium current: each spike generates a small amount of calcium influx that adds to the intracellular calcium concentration so that the potassium current is incremented accordingly. We stress that the randomness of the voltage crossing times due to the diffusion in membrane potential equation causes randomness of the initial calcium concentration, so that in the present model both equations are stochastic.

The proposed model is described in Section 2. Some quantitative results, specifically relating the mean firing rate to the mean calcium concentration and the corresponding asymptotic relationships are reported in Section 3. Finally, Section 4 is devoted to the description of the simulation algorithm and to the discussion of numerical results. Section 5 concludes and points to possible developments.

2. **The model.** The diffusive approximation for a LIF model with synaptic currents (excitatory and inhibitory) of homogeneous Poisson type is governed by: (i) the Equation

$$dV(\tau) = -\frac{g_{\mathrm{L}}}{C_{\mathrm{m}}}\left[V(\tau) - V_{\mathrm{rest}}\right]d\tau + \mu d\tau + \sigma dW(\tau) \qquad (\tau \geq \tau_0), \tag{1}$$

with initial condition $V(\tau_0) = V_{\mathrm{reset}}$ (see Eqs. (15) and related observation; Eqs. (21) in [8]); (ii) the presence of a threshold value V_{th} for the membrane potential $V(\tau)$ that, once attained, produces an action potential (spike); (iii) the reset mechanism for the membrane potential on the value V_{reset}. In Eq. (1) $W(\tau)$ is a standard Wiener process, C_{m} represents the membrane capacitance, g_{L} the leak membrane

conductance and $V_{\rm rest}$ the resting membrane potential. Moreover, the parameters μ and σ are such that $V_{\rm rest} + \mu C_{\rm m}/g_{\rm L}$ and $\sigma^2 C_{\rm m}/(2g_{\rm L})$ represent the asymptotic values for the mean and the variance, respectively, of the free membrane potential. Indeed, referring to homogeneous Poisson processes for excitation and inhibition, it results

$$\mu := a_{\rm E}\lambda_{\rm E} - a_{\rm I}\lambda_{\rm I}; \qquad \sigma^2 := a_{\rm E}^2\lambda_{\rm E} + a_{\rm I}^2\lambda_{\rm I},$$

where $a_{\rm E}$ and $a_{\rm I}$ represent the unitary increments and decrements and $\lambda_{\rm E}$, $\lambda_{\rm I}$ the corresponding arrival rates, so that the synaptic current is

$$I_{\rm syn}(\tau) = C_{\rm m}\mu + C_{\rm m}\sigma\frac{dW(\tau)}{d\tau}.$$

Here, along the lines of Liu and Wang [22], we consider explicitly the role of the potassium ion channel whose conductance $g_{\rm AHP}$ is assumed to be proportional to the instantaneous calcium concentration: $g_{\rm AHP}(\tau) = \beta_{\rm AHP}[{\rm Ca}^{2+}](\tau)$. Then, the current generated by the potassium channel is

$$I_{\rm AHP}(\tau) = \beta_{\rm AHP}[{\rm Ca}^{2+}](\tau)[V(\tau) - V_{\rm K}]$$

where $V_{\rm K}$ represents the reversal potential of the potassium channel. Furthermore, the calcium concentration decays exponentially with its characteristic time $\tau_{\rm Ca}$ while each spike generates a calcium influx α.

Therefore, the proposed model for the generation of a spike train is described by the Equations:

$$dV(\tau) = -\frac{g_{\rm L}}{C_{\rm m}}\left[V(\tau) - V_{\rm rest}\right]d\tau - \frac{I_{\rm AHP}(\tau)}{C_{\rm m}}d\tau + \frac{I_{\rm syn}(\tau)}{C_{\rm m}}d\tau \qquad (\tau \geq \tau_0), \tag{2}$$

$$\frac{d[{\rm Ca}^{2+}](\tau)}{d\tau} = -\frac{1}{\tau_{\rm Ca}}[{\rm Ca}^{2+}](\tau) \tag{3}$$

with the *reset mechanism*,[1]

$$\text{if } \tau_{\rm f} : V(\tau_{\rm f}^-) = V_{\rm th} \quad \text{then} \quad V(\tau_{\rm f}^+) = V_{\rm reset}, \quad [{\rm Ca}^{2+}](\tau_{\rm f}^+) = [{\rm Ca}^{2+}](\tau_{\rm f}^-) + \alpha, \quad \text{and} \quad \tau_{\rm f} = \tau_0. \tag{4}$$

For motivations and consequences of such assumptions see again Liu and Wang [22]; see also La Camera [21], where a different repositioning mechanism is considered.

Remark 1. With respect to Eq. (1), the resting membrane potential $V_{\rm rest}$ and the leakage conductance $g_{\rm L}$ should be renamed since we excluded from these parameters the contribution of the potassium channel, expressed in terms of $V_{\rm K}$ and $g_{\rm AHP}$; however, for readability we maintain the previous notation. ◁

Remark 2. As shown in Eq. (4), the term "reset" is a misnomer for the calcium concentration: at the beginning of each ISI it is a random variable $\mathcal{Y}$ function of the already observed spikes. In this regard we find useful to use two different letters to indicate the time: τ (for the dynamics of a single ISI) that is reset after each spike, and t (for the entire spike train) that goes until the saturation of calcium level. Obviously $t - \tau$ coincides with the sum of ISIs already occurred. Furthermore, $t_0 = \tau_0$ and the effective value of calcium concentration, at the beginning of each spike train, is not considered significant, i.e. $[{\rm Ca}^{2+}](t_0) = 0$. ◁

[1] As usual the superscripts $-$ and $+$ denote left and right limits, respectively.

By setting

$$Y(\tau) := [\mathrm{Ca}^{2+}](\tau); \qquad \theta_{\mathrm{L}} := C_{\mathrm{m}}/g_{\mathrm{L}}, \quad \rho := V_{\mathrm{rest}}, \quad \gamma := C_{\mathrm{m}}/\beta_{\mathrm{AHP}},$$

Eq. (2) becomes

$$dV(\tau) = -\left[\frac{V(\tau)-\rho}{\theta_{\mathrm{L}}} + \frac{V(\tau)-V_{\mathrm{K}}}{\gamma}Y(\tau) - \mu\right]d\tau + \sigma dW(\tau) \qquad (\tau \geq \tau_0),$$

and finally, by setting

$$\Theta_{\mathrm{L}}(\tau) := \frac{\theta_{\mathrm{L}}}{1+\theta_{\mathrm{L}}Y(\tau)/\gamma}, \qquad P(\tau) := \left[\frac{\rho}{\theta_{\mathrm{L}}} + \frac{V_{\mathrm{K}}}{\gamma}Y(\tau)\right]\Theta_{\mathrm{L}}(\tau), \tag{5}$$

it can be rewritten as

$$dV(\tau) = -\left[\frac{V(\tau)-P(\tau)}{\Theta_{\mathrm{L}}(\tau)} - \mu\right]d\tau + \sigma dW(\tau) \qquad (\tau \geq \tau_0). \tag{6}$$

We stress that in Eq. (6) the calcium concentration $Y(\tau)$, the passive membrane time constant $\Theta_{\mathrm{L}}(\tau)$ and the resting membrane potential $P(\tau)$ represent stochastic processes.

To choose suitable values for the involved parameters we followed the indications given by several authors for cortical regular spiking pyramidal neurons: $V_{\mathrm{rest}} = 0$,[2] $V_{\mathrm{th}} = 16$ mV, $V_{\mathrm{reset}} = 10$ mV, $V_{\mathrm{K}} = -10$ mV, $\tau_{\mathrm{Ca}} = 500$ ms, $\theta_{\mathrm{L}} = 20$ ms, $\alpha = 0.2$ μM, $\gamma = 150$ ms$\cdot\mu$M, $\mu \in (0.4, 0.8)$ mV/ms and $\sigma^2 = 1$ mV^2/ms. In the sequel, for brevity, these settings will be indicated by the expression *considered parametric configuration*.

3. **Adaptation quantitative features.** Eq. (6) defines a generalized OU process already considered by Buonocore *et al.* [5, 6]. The analysis of the model described via Eqs. (3), (4) and (6) is made more complex by the stochastic nature of the calcium concentration; however, the change in calcium concentration is slow compared with the evolution of the membrane potential. Hence we can apply a fast-slow variable analysis ([22] and references therein) where the slower calcium dynamics can be solved by averaging over the faster voltage subsystem.

In the following we outline the steps of the devised procedure. It is quite evident that the mean firing rate is a decreasing function of the calcium concentration. Then, to derive an empirical relationship between these two quantities, we observe that in the case of constant deterministic calcium concentration y, i.e. when Eq. (4) reduces to $[\mathrm{Ca}^{2+}](\tau) = y$, Eq. (6) describes the evolution of the potential membrane $\tilde{V}(t)$ as a standard LIF model with passive membrane time constant and reset membrane potential given by Eq. (5) with $Y(\tau)$ replaced by y. On the other hand, the corresponding firing rate $f(y)$ can be obtained as the reciprocal of the mean first passage time (FPT) of the process $\tilde{V}(\tau)$ through V_{th} having y as calcium concentration: $\tau_1(y) := \mathbb{E}\left[T_{\tilde{V},V_{\mathrm{th}}}(V_{\mathrm{reset}}, \tau_0; y)\right]$. By applying a version with rescaled parameter of the formula (6.a) in [24] we numerically evaluate $\tau_1(y)$ for a suitable range of fixed values y, coherent with the adaptation phenomenon (y ranging from 0 to a few units of the calcium concentration influx α), whose reciprocal $f(y)$ quite remarkably fits a quadratic relationship:

$$f(y) = f_0 + f_1 y + f_2 y^2, \tag{7}$$

[2]So that the values for the membrane potential and the firing threshold are rescaled with respect to the real value of the rest potential.

where $f_0 > 0$, $f_1 < 0$ and $f_2 \geq 0$. For $\mu = 0.8$ mV/ms, part (a) of Figure 1 confirms

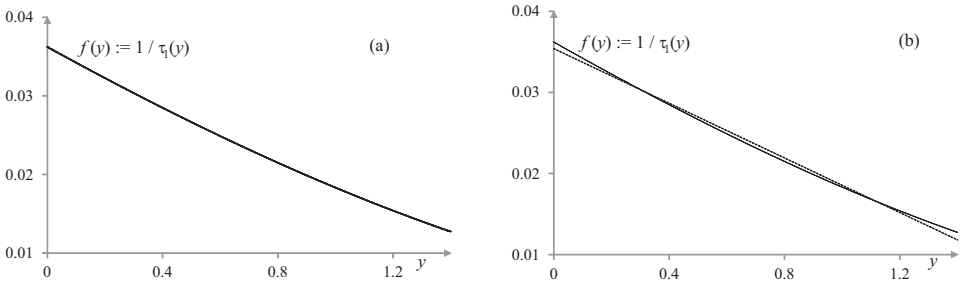

FIGURE 1. For the considered parametric configuration with $\mu = 0.8$ mV/ms: part (a) shows the plot of the calculated (by means of Eq. (6.a) in [24]) mean firing rate $f(y)$ as a function of calcium concentration y and its quadratic trend line (they are overlapped); part (b) shows again the plot of the calculated mean firing rate (solid line) and its linear trend line (dotted line). $\tau_1(y)$ indicates mean first passage time of membrane potential through firing threshold in the case of degenerate Eq. (3): $Y(\tau) \equiv y$. Firing rate in ms^{-1} and calcium concentration in μM.

the goodness of the quadratic relationship in the considered range of the calcium concentration; in such an interval the two curves are essentially overlapped with absolute error of order 10^{-3}. As a comparison, part (b) of the same figure outlines that a linear relationship is unable to reproduce the firing rates in particular at the ends of the considered range of calcium concentration, where the relative error is about 100 times greater than the one obtained by the quadratic approximation. The difference in the goodness of fit between the two trend lines (quadratic and linear) decreases for smaller values of μ (not shown).

Now we consider the mean $m_Y(t) := \mathbb{E}[Y(t)]$ of the process $Y(t)$. Averaging over the fast dynamics of the membrane potential $V(t)$, the mean calcium influx at time t is given by $\alpha f(t) \equiv \alpha f[m_Y(t)]$ and the evolution equation for the slow variable $m_Y(t)$ becomes

$$\dot{m}_Y = \alpha f - \frac{m_Y}{\tau_{\text{Ca}}}, \tag{8}$$

that together with the quadratic relationship (7) leads to:

$$\dot{m}_Y = \alpha f_0 + \left(\alpha f_1 - \frac{1}{\tau_{\text{Ca}}}\right) m_Y + \alpha f_2 m_Y^2.$$

The latter is a Riccati Equation with constant coefficients, whose general solution is easily obtained as

$$m_Y(t) = \alpha f_0 \frac{1 - e^{-\sqrt{\Delta}\ t}}{\lambda_2 e^{-\sqrt{\Delta}\ t} - \lambda_1}, \tag{9}$$

where $\lambda_1 \leq \lambda_2 < 0$ and Δ represent the eigenvalues and the discriminant of the associated equation, respectively:

$$\lambda_{1,2} = \frac{1}{2}\left(\alpha f_1 - \frac{1}{\tau_{\text{Ca}}} \mp \sqrt{\Delta}\right); \qquad \Delta = \left(\alpha f_1 - \frac{1}{\tau_{\text{Ca}}}\right)^2 - 4\alpha^2 f_0 f_2 > 0.$$

From Eqs. (7) and (9) we obtain the expression for the instantaneous firing rate $f(t)$:

$$f(t) = f_0 + f_1 m_Y(t) + f_2 m_Y^2(t). \tag{10}$$

Since

$$y_{\rm ss} := \lim_{t\to\infty} m_Y(t) = -\alpha f_0 \frac{1}{\lambda_1}, \tag{11}$$

we find

$$f_{\rm ss} := f_0 + f_1 y_{\rm ss} + f_2 y_{\rm ss}^2 = f_0 \left(1 - \frac{\alpha f_1}{\lambda_1} + \frac{\alpha^2 f_0 f_2}{\lambda_1^2}\right). \tag{12}$$

So, the resulting degree of adaptation is:

$$F_{\rm adap} := \frac{f_0 - f_{\rm ss}}{f_0} \equiv 1 - \frac{f_{\rm ss}}{f_0} = \frac{\alpha}{\lambda_1}\left(f_1 - \frac{\alpha f_0 f_2}{\lambda_1}\right). \tag{13}$$

For the determination of the adaptation time constant $\tau_{\rm adap}$ it is useful to note that in the steady state the variation of the calcium is null and thus from Eq. (8) a straightforward relationship between $y_{\rm ss}$ and $f_{\rm ss}$ can be obtained

$$y_{\rm ss} = \alpha \tau_{\rm Ca} f_{\rm ss};^{3} \tag{14}$$

then, from it and Eqs. (11) it follows:

$$\frac{f_{\rm ss}}{f_0} = \frac{-1/\lambda_1}{\tau_{\rm Ca}}.$$

Finally, by the relation $f_{\rm ss}/f_0 = \tau_{\rm adap}/\tau_{\rm ca}$ proved in [22], the adaptation time constant is:

$$\tau_{\rm adap} = -\frac{1}{\lambda_1}. \tag{15}$$

Remark 3. As $f_2 \to 0^+$ one has $\lambda_2 \to 0^-$, $\lambda_1 \to \tilde{\lambda}_1 := \alpha f_1 - 1/\tau_{\rm Ca}$ and $-\sqrt{\Delta} \to \tilde{\lambda}_1$ so that

$$\tilde{m}_Y(t) = -\frac{\alpha f_0}{\tilde{\lambda}_1}\left(1 - e^{\tilde{\lambda}_1 t}\right), \qquad \tilde{f}(t) = f_0 - \frac{\alpha f_0 f_1}{\tilde{\lambda}_1}\left(1 - e^{\tilde{\lambda}_1 t}\right), \tag{16}$$

and finally we obtain

$$\tilde{y}_{\rm ss} = -\alpha f_0 \frac{1}{\tilde{\lambda}_1}, \quad \tilde{f}_{\rm ss} = f_0\left(1 - \frac{\alpha f_1}{\tilde{\lambda}_1}\right), \quad \tilde{\tau}_{\rm adap} = -\frac{1}{\tilde{\lambda}_1}, \quad \tilde{F}_{\rm adap} = \frac{\alpha f_1}{\tilde{\lambda}_1}, \tag{17}$$

as the asymptotic mean calcium concentration, the asymptotic mean firing rate, the adaptation time constant and the degree of adaptation, respectively.[4] ◁

4. **ISIs generation and numerical results.** To validate Eqs. (9) and (10) (and related Eqs. (11)–(17)) we generate N spike trains for a time interval long enough to yield some dozens of spikes in each one of them. In order to obtain a single spike train we utilized the hazard rate method, based on a hazard rate function numerically evaluated.

Specifically, let $\mathcal{Y}$ be the calcium concentration at the beginning of a single ISI (see, also, Remark 2) and let $T_{V,V_{\rm th}}(V_{\rm reset}, \tau_0; \nu)$ be the first passage time of $V(t)$ through $V_{\rm th}$ known that (i) $V(\tau_0) = V_{\rm reset}$ and (ii) $\mathcal{Y} = \nu$. In this specific context, $T_{V,V_{\rm th}}(V_{\rm reset}, \tau_0; \nu)$ also represents the interspike interval that starts having ν as initial calcium concentration. We now denote with $g_V(V_{\rm th}, \tau | V_{\rm reset}, \tau_0; \nu)$ and

[3] Obviously Eq.(14) is directly verified by means of Eqs. (11) and (12).

[4] Note that these expressions are equivalent to the ones reported in [22], where the firing rate is directly assumed linearly dependent on the calcium concentration.

$G_V(V_{\rm th},\tau|V_{\rm reset},\tau_0;\nu)$ the probability density function (pdf) and the distribution function of $T_{V,V_{\rm th}}(V_{\rm reset},\tau_0;\nu)$, respectively. Then, the following integral equation holds:

$$\psi_V(V_{\rm th},\tau|V_{\rm reset},\tau_0;\nu)=\int_{\tau_0}^{\tau}\psi_V(V_{\rm th},\tau|V_{\rm th},s;\nu)g_V(V_{\rm th},s|V_{\rm reset},\tau_0;\nu)\,ds. \tag{18}$$

The kernel in Eq. (18) is the probability current with removed singularity (see, for instance, [7]and [11]) and efficient quadrature formulas can be used to approximate the unknown $g_V(V_{\rm th},\tau|V_{\rm reset},\tau_0;\nu)$; with a further quadrature we also get the function $G_V(V_{\rm th},\tau|V_{\rm reset},\tau_0;\nu)$. Thereafter, the hazard rate function of $T_{V,V_{\rm th}}(V_{\rm reset},\tau_0;\nu)$,

$$\lambda_V(\tau;\nu):=\frac{g_V(V_{\rm th},\tau|V_{\rm reset},\tau_0;\nu)}{1-G_V(V_{\rm th},\tau|V_{\rm reset},t_0;\nu)}\qquad(\tau\ge\tau_0), \tag{19}$$

can be easily evaluated: directly on the same mesh of the used quadrature formula and by means of interpolation on other values of its argument.

A sketch of the used algorithm is provided in the framed box below. Note that Λ is an upper bound for the hazard rate function $\lambda_V(\tau;\nu>0)$ since the neuron during the first ISI of any spike train is not affected by the adaptation mechanism. The algorithm saves all the values assumed by the random variable $\mathcal{Y}$ and all the generated ISIs from which, by summation, the spike train $t_1,t_2,\dots$ is obtained.

As shown in [4], this algorithm outperforms the classical methods based on trajectories reconstruction (such as the Euler-Maruyama method) in accuracy; in the case of low firing rates (subthreshold regime) also its efficiency is considerably higher. Moreover, in any situation it is not affected by the systematic bias (overestimation of crossing times) that affects these methods.

HRM-Algorithm for generating a spike train

1. Determine an upper bound Λ of $\lambda_V(\tau;0)$.
2. $t\leftarrow t_0$ and $\nu\leftarrow 0$; set $t_{\max}$.
3. Numerically evaluated $\lambda_V(\tau;\nu)\quad(\tau_0\le\tau\le t_{\max})$.
4. $\quad\tau_{\rm f}\leftarrow\tau_0$; $m\leftarrow 0$; $z_0\leftarrow 1$; $u_0\leftarrow 1$.
5. $\quad\quad m\leftarrow m+1$.
6. $\quad\quad$ Get a random number z_m by Z_m with $Z_m\overset{d}{=}\mathrm{Exp}(\Lambda)$ independent from $\sigma(Z_0,\dots,Z_{m-1})$.
7. $\quad\quad\tau_{\rm f}\leftarrow\tau_{\rm f}+z_m$.
8. $\quad\quad$ Get a random number u_m by $U_m\overset{d}{=}\mathrm{U}(0,1)$ independent from Z_m and $\sigma(U_0,\dots,U_{m-1})$.
9. $\quad\quad$ if $\dfrac{\lambda_V(\tau_{\rm f};\nu)}{\Lambda}<u_m$ return to `step` 5.
10. $\quad I\leftarrow\tau_{\rm f}-\tau_0$; save I; $t\leftarrow t+I$.
11. $\quad\nu\leftarrow Y(t)+\alpha$; save ν.
12. $\quad$ if $t<t_{\max}$ return to `step` 3.

The symbols $\overset{d}{=}$, $\mathrm{Exp}(\cdot)$, $U(\cdot)$ and $\sigma(\cdot)$ indicate the equality in distribution, the exponential distribution, the uniform absolutely continue distribution and the generated σ-algebra, respectively.

By each one of the generated spike trains, a sample path $y(t)$ of the process $Y(t)$, can be obtained as

$$y_j(t)=\alpha\sum_{i=1}^{k}e^{-\frac{t-t_{j,i}}{\tau_{\rm Ca}}}\qquad(t_{j,k}\le t\le t_{j,k+1},\ \text{and}\ j=1,2,\dots,N), \tag{20}$$

so that the corresponding sample mean $\hat{m}_Y(t)$ is an estimator for $m_Y(t)$. The left hand side of Figure 2 compares the plot of the instantaneous mean calcium

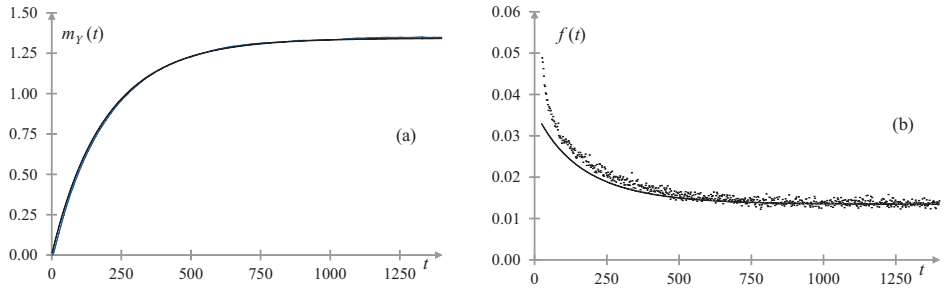

FIGURE 2. For the considered parametric configuration with $\mu = 0.8$ mV/ms: part (a) shows plots of $m_Y(t)$ (solid line) evaluated via Eq. (9) and its estimate $\hat{m}_Y(t)$ (dotted line) — time in ms and calcium concentration in μM—; part (b) shows plots of the mean firing rate $f(t)$ (solid line) from Eq. (10) and its trial estimated counterpart (dots) —firing rate in ms^{-1}.

concentration as evaluated by Eq. (9) to $\hat{m}_Y(t)$. On the right part of the same Figure, the plot of the instantaneous mean firing rate as obtained by Eq. (10) is compared to its trial–averaged estimate (considered time interval subdivided in 2 ms time bins). The agreement between estimates and function seems quite satisfactory; the same conclusion holds for several values of $\mu \in (0.4, 0.8)$ mV/ms (for brevity, figures not reported here). Quadrature mesh, $h = \theta/10$, and sample size, $N = 10000$, have been chosen to balance results accuracy and computational times. As a confirmation of the improvement, Figure 3 compares plots of $\tilde{m}_Y(t)$ in Remark 3 with $\hat{m}_Y(t)$.

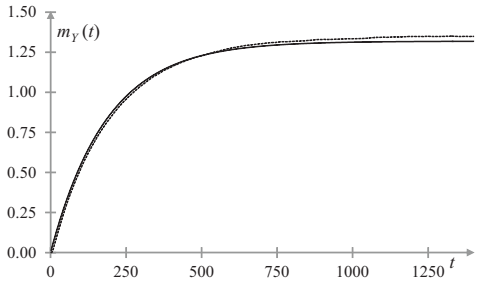

FIGURE 3. For the considered parametric configuration with $\mu = 0.8$ mV/ms plots of $\tilde{m}_Y(t)$ (solid line) evaluated via Eq. (16) and its estimate $\hat{m}_Y(t)$ (dotted line) — time in ms and calcium concentration in μM. Note, in particular, the larger error of the stationary mean calcium concentration $\tilde{y}_{ss}$ with respect to y_{ss}: relative error about $2.5 \cdot 10^{-2}$ versus $5 \cdot 10^{-3}$.

In order to devise an approximation of the ISI pdf, we proceed as follows. We recall that $\mathcal{Y}$ denotes the calcium concentration at the beginning of each ISI in the

current spike train. Let $f_{\mathcal{Y}}(\nu)$, $g(\tau)$ denote the pdfs of $\mathcal{Y}$ and of the generic ISI, respectively.[5] Then, setting $g(\tau|\nu) \equiv g_V(V_{\text{th}}, \tau|V_{\text{reset}}, \tau_0; \nu)$, the function $g(\tau)$ can be obtained by averaging $g(\tau|\nu)$ with respect to $f_{\mathcal{Y}}(\nu)$:

$$\begin{aligned} g(\tau) = \mathbb{E}_{f_{\mathcal{Y}}}\left[g(\tau|\nu)\right] = g(\tau|0)\mathbb{P}(\mathcal{Y}=0) + g(\tau|\alpha)\mathbb{P}(\mathcal{Y}=\alpha) \\ + \int_{\alpha}^{+\infty} g(\tau|\nu) f_{\mathcal{Y}}(\nu) d\nu \qquad (\tau \geq \tau_0). \end{aligned} \tag{21}$$

With regards to the discrete part of $\mathcal{Y}$ distribution we can resort to the values of ν stored during the N spike trains generation; while the integral in the right–side of (21) can be evaluated by means of a suitable quadrature rule:[6]

$$\int_{\alpha}^{+\infty} g(\tau|\nu) f_{\mathcal{Y}}(\nu) d\nu \approx \sum_{l=1}^{r} w_l \cdot g(\tau|\nu_l) f_{\mathcal{Y}}(\nu_l). \tag{22}$$

To evaluate $f_{\mathcal{Y}}(\nu_l)$, for $l = 1, 2, \ldots, r$, we can proceed at least in two different ways. First, it is useful to observe that the nodes subdivide the support of $\mathcal{Y}$ in r classes; then, the values of ν saved during the N spike trains generation provide a sample $(\nu_1, \nu_2, \ldots, \nu_M)$ of size M sufficient to employ the relative frequencies of each class:

$$\tilde{f}_{\mathcal{Y}}(\nu_l) = \frac{n_l}{M \cdot b_l} \qquad (l = 1, 2, \ldots, r). \tag{23}$$

Here b_l represents the width of l-th class and n_l the related absolute frequency.

As an alternative (Bayesian) way, we can initially assume that $\mathcal{Y}$ is uniformly distributed after α and then we can update its pdf according to a generated ISI sample, $\boldsymbol{\tau} = (\tau_1, \tau_2, \ldots, \tau_n)$. For this purpose, we can take $n = N$ and τ_j a randomly chosen ISI in the j-th spike train; clearly, the first two ISIs of each spike train corresponding to $\nu = 0$ and $\nu = \alpha$ must be discarded before sampling.[7] Therefore, with obvious meaning of symbols, one has:

$$\tilde{f}_{\mathcal{Y}}(\nu_l) \equiv f_{\mathcal{Y}}(\nu_l|\boldsymbol{\tau}) = C \prod_{j=1}^{n} g(\tau_j|\nu_l) \qquad (l = 1, 2, \ldots, r). \tag{24}$$

The constant C is the normalizing factor of the absolutely continuous part of $\mathcal{Y}$. The results obtained by means of Eq. (24) require a higher computational time with respect to.

Figure 4 shows the agreement between the pdf $g(\tau)$, evaluated by means of Eqs. (21)–(23), and the corresponding frequency polygon.

5. **Concluding remarks.** In this work we modeled the spike-frequency adaptation phenomenon by a generalization of the LIF model where the evolution of the membrane potential is affected by the calcium dynamics that activate a potassium current. Then we fit the relationship between the mean calcium concentration and the mean firing rate; by a fast-slow variable analysis we were able to solve the slow calcium dynamics and obtain analytical expressions describing the quantities of interest. Finally, to confirm such analytical results, we suitably modified the hazard rate method to generate spike trains and so to estimate the interspike intervals

[5] Indeed the random variable $\mathcal{Y}$ has a probability mass concentrated in 0 and α and it is absolutely continuous after α.

[6] Here, r denotes the number of nodes of quadrature, $\{\nu_1, \nu_2, \ldots, \nu_r\}$ and $\{w_1, w_2, \ldots, w_r\}$ the related nodes and weights, respectively.

[7] We stress that the size n of the sample $\boldsymbol{\tau}$ loses a unit corresponding to those generated spike trains with less than two ISIs.

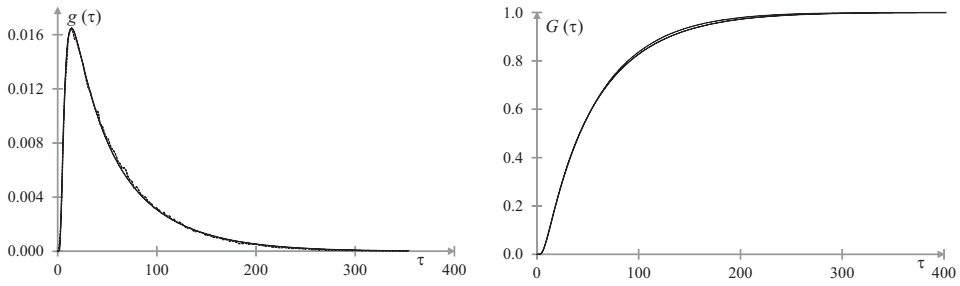

FIGURE 4. For the considered parametric configuration with $\mu = 0.8$ mV/ms: on the left hand side plots of $g(\tau)$ (solid line) evaluated via Eqs. (21)–(23) and its estimated counterpart via spike trains generation (dotted line); on the right hand side plots of the corresponding distribution function $G(\tau)$ (solid line) and its estimated counterpart via spike trains generation (dotted line).

density. These numerical experiments gave results in very good agreement with the analytical estimates. To obtain such estimates, in particular for the ISIs pdf, we adopted an integrated approach that combines numerical and simulation techniques with a theoretical study. Further developments should include the estimation of the calcium concentration at the beginning of each ISI without resorting to generations methods; however, in the authors' opinion, this is a very challenging task due to the dependence of the calcium level on the entire past history of the process.

Acknowledgments. The authors would like to thank the anonymous reviewers, whose comments really help to improve the manuscript. This work was partially supported by a GNCS-INDAM (Gruppo Nazionale per il Calcolo Scientifico) research grant.

REFERENCES

[1] J. Benda and A. W. M. Herz, A universal model for spike-frequency adaptation, *Neural Computation*, **15** (2003), 2523–2564.
[2] R. Brette and W. Gerstner, Adaptive exponential integrate-and-fire model as an effective description of neuronal activity, *Journal of Neurophysiology*, **94** (2005), 3637–3642.
[3] D. A. Brown and P. R. Adams, Muscarinic supression of a novel voltage-sensitive K+ current in a vertebrate neuron, *Nature*, **183** (1980), 673–676.
[4] A. Buonocore, L. Caputo, E. Pirozzi and M. F. Carfora, A simple algorithm to generate firing times for leaky integrate-and-fire neuronal model, *Mathematical Biosciences and Engineering*, **11** (2014), 1–10.
[5] A. Buonocore, L. Caputo, E. Pirozzi and L. M. Ricciardi, On a generalized leaky integrate-and-fire model for single neuron activity, in *Computer Aided Systems Theory - EUROCAST 2005*, Lecture Notes in Computer Science, 5717, Springer, Berlin-Heidelberg, 2009, 152–158.
[6] A. Buonocore, L. Caputo, E. Pirozzi and L. M. Ricciardi, On a stochastic leaky integrate-and-fire neuronal model, *Neural Computation*, **22** (2010), 2558–2585.
[7] A. Buonocore , A. G. Nobile and L. M. Ricciardi, A new integral equation for the evaluation of first-passage-time probability densities, *Advances in Applied Probability*, **19** (1987), 784–800.
[8] A. N. Burkitt, A review of the integrate-and-fire neuron model: I. Homogeneous synaptic input, *Biological Cybernetics*, **95** (2006), 1–19.
[9] M. J. Chacron, K. Pakdaman and A. Longtin, Interspike interval correlations, memory, adaptation, and refractoriness in a leaky integrate-and-fire model with threshold fatigue, *Neural Computation*, **15** (2003), 253–278.

[10] S. M. Crook, G. B. Ermentrout and J. M. Bower, Spike frequency adaptation affects the synchronization properties of networks of cortical oscillators, *Neural Computation*, **10** (1998), 837–854.
[11] Y. Dong, F. Mihalas and E. Niebur, Improved integral equation solution for the first passage time of leaky integrate-andfire neurons, *Neural Computation*, **23** (2011), 421–434.
[12] B. Ermentrout, M. Pascal and B. Gutkin, The effects of spike frequency adaptation and negative feedback on the synchronization of neural oscillators, *Neural Computation*, **13** (2001), 1285–1310.
[13] I. A. Fleidervish, A. Friedman and M. J. Gutnick, Slow inactivation of Na+ current and slow cumulative spike adaptation in mouse and guinea-pig neocortical neurones in slices, *The Journal of Physiology*, **493** (1996), 83–97.
[14] G. Fuhrmann, H. Markram and M. Tsodyks, Spike frequency adaptation and neocortical rhythms, *Journal of Neurophysiology*, **88** (2002), 761–770.
[15] R. Granit, D. Kernell and G. K. Shortess, Quantitative aspects of repetitive firing of mammalian motoneurones, caused by injected currents, *The Journal of Physiology*, **168** (1963), 911–931.
[16] B. Hille, *Ion Channels of Excitable Membranes*, Sinauer Associates, Sunderland, MA, 2001.
[17] A. L. Hodgkin and A. F. Huxley, A quantitative description of membrane current and its application to conduction and excitation in nerve, *Journal of Physiology*, **117** (1952), 500–544.
[18] A. V. Holden, *Models of the Stochastic Activity of Neurones*, Springer-Verlag, New York, 1976.
[19] R. Jolivet, R. Kobayashi, A. Rauch, R. Naud, S. Shinomoto and W. Gerstner, A benchmark test for a quantitative assessment of simple neuron models, *Journal of Neuroscience Methods*, **169** (2008), 417–424.
[20] R. Kobayashi, Y. Tsubo and S. Shinomoto, Made-to-order spiking neuron model equipped with a multi-timescale adaptive threshold, *Frontiers in Computational Neuroscience*, **3** (2009), p9.
[21] G. La Camera, A. Rauch, H. R. Luescher, W. Senn and S. Fusi, Minimal models of adapted neuronal response to in vivo-like input currents, *Neural Computation*, **16** (2004), 2101–2124.
[22] Y. H. Liu and X. J. Wang, Spike-frequency adaptation of a generalized leaky integrate-and-fire model neuron, *Journal of Computational Neuroscience*, **10** (2001), 24–45.
[23] D. V. Madison and R. A. Nicoll, Control of the repetitive discharge of rat CA1 pyramidal neurones in vitro, *The Journal of Physiology*, **354** (1984), 319–331.
[24] A. G. Nobile, L. M. Ricciardi and L. Sacerdote, Exponential trends of Ornstein-Uhlenbeck first-passage-time densities, *Journal of Applied Probability*, **22** (1985), 360–369.
[25] R. K. Powers, A. Sawczuk, J. R. Musick and M. D. Binder, Multiple mechanisms of spike-frequency adaptation in motoneurones, *Journal of Physiology*, **93** (1999), 101–114.
[26] A. Rauch, G. La Camera, H. R. Luescher, W. Senn and S. Fusi, Neocortical cells respond as integrate-and-fire neurons to in vivo-like input currents, *Journal of Neurophysiology*, **90** (2003), 1598–1612.
[27] L. Sacerdote and M. Giraudo, Stochastic integrate and fire models: A review on mathematical methods and their applications, in *Stochastic Biomathematical Models with Applications to Neuronal Modeling* (eds. Bachar, Batzel and Ditlevsen), Lecture Notes in Mathematics 2058, Springer, Berlin-Heidelberg (2013), 99–148.
[28] P. Sah, Ca2+-activated K+ currents in neurones: Types, physiological roles and modulation, *Trends in Neurosciences*, **19** (1996), 150–154.
[29] S. Shinomoto, Y. Sakai and S. Funahashi, The Ornstein-Uhlenbeck process does not reproduce spiking statistics of neurons in prefrontal cortex, *Neural Computation*, **11** (1999), 935–951.
[30] W. R. Softky and C. Koch, The highly irregular firing of cortical cells is inconsistent with temporal integration of random EPSPs, *Journal of Neurosciences*, **13** (1993), 334–350.
[31] H. C. Tuckwell, *Introduction to Theoretical Neurobiology, Vol. 2*, Cambridge University Press, Cambridge, England, 1988.

Received April 01, 2015; Accepted November 01, 2015.

E-mail address: aniello.buonocore@unina.it
E-mail address: luigia.caputo@unina.it
E-mail address: enrica.pirozzi@unina.it
E-mail address: f.carfora@na.iac.cnr.it